^{99m}Tc-HYNIC-Gastrin Peptides: Assisted Coordination of ^{99m}Tc by Amino Acid Side Chains Results in Improved Performance Both In Vitro and In Vivo

Robert King[1], M. Bashir-Uddin Surfraz[2], Ciara Finucane[1], Stefano C.G. Biagini[3], Philip J. Blower[4], and Stephen J. Mather[1]

[1]Centre for Molecular Oncology and Imaging, Barts and the London School of Medicine, John Vane Science Centre, London, United Kingdom; [2]Cancer Research Group, Biosciences Department, University of Kent, Canterbury, United Kingdom; [3]Functional Materials Group, School of Physical Sciences, University of Kent, Canterbury, United Kingdom; and [4]Division of Imaging Sciences, Kings College London, Rayne Institute, St. Thomas' Hospital, London, United Kingdom

The aim of this study was to determine the effects of assisted coordination by amino acids such as histidine and glutamic acid on the function of ^{99m}Tc-labeled gastrin peptide–hydrazinonicotinamide (HYNIC) conjugates and their ability to target cholecystokinin-R in small-animal models. **Methods:** Three peptide–HYNIC conjugates containing the -AYGWMDF-NH2 C-terminal sequence and combinations of histidine, glutamic acid, and glycine were synthesized, radiolabeled with ^{99m}Tc/^{99}Tc using either tricine or ethylenediaminediacetic acid as a coligand, and analyzed by the high-performance liquid chromatography and liquid chromatography–mass spectrometric techniques. Stability, receptor binding, and internalization and in vivo targeting in AR42J-bearing mice were assessed. **Results:** When radiolabeling was performed using tricine as a coligand, the insertion of a histidine residue near the HYNIC residue resulted in the displacement of one molecule of tricine from the coordination sphere, a reduction in the number of radiolabeled species formed, an improvement in the in vitro stability, an increase in the rate of radiopeptide internalization, and a significant improvement in tumor uptake in vivo. When radiolabeling was performed using ethylenediaminediacetic acid as a coligand, no effect on coligand binding, homogeneity, or in vitro stability was observed but a significant improvement in the internalization in vitro and tumor uptake in vivo was again found. All of the complexes formed showed similar receptor affinity in competitive radioligand binding assays. **Conclusion:** The insertion of histidine into the sequence of peptide–HYNIC conjugates can result in more stable, more homogeneous complexes that show improvements in tumor-targeting performance both in vitro and in vivo.

Key Words: molecular imaging; radiopharmaceuticals; peptides; HYNIC; coordination; technetium

J Nucl Med 2009; 50:591–598
DOI: 10.2967/jnumed.108.058289

Received Sep. 19, 2008; revision accepted Dec. 19, 2008.
For correspondence or reprints contact: Stephen J. Mather, St. Bartholomew's Hospital, Charterhouse Square, London, EC1M 6BQ, U.K.
E-mail: s.j.mather@qmul.ac.uk

Because of its ease and flexibility of use and the attractive characteristics of the resulting radiotracers, hydrazinonicotinamide (HYNIC) has become a popular bifunctional complexing agent for labeling peptides and proteins with ^{99m}Tc (*1–3*). HYNIC satisfies only part of the coordination requirements of the radiometal, and additional coligands must be incorporated to complete the coordination sphere (*4,5*). The ability to vary these coligands, and consequently the physicochemical properties of the complexes formed, is a useful characteristic of this labeling system (*6–8*). The 2 most widely used coligands are tricine and ethylenediaminediacetic acid (EDDA) (*3*). EDDA forms complexes that have been shown to be stable both in vitro and in vivo, but the formation of these compounds requires heating during the labeling procedure, which limits the use of the procedure for larger polypeptides with tertiary structures that would be disrupted by heating. Tricine, on the other hand, labels efficiently and rapidly at room temperature but forms complexes with generally lower stability and poorer performance in vivo. In addition, high-performance liquid chromatography (HPLC) analysis of peptides labeled with tricine invariably shows the presence of multiple radioactive species, arising from isomerism in the technetium coordination sphere and varying numbers of coligands present (*3*). Therefore, a need exists to improve the characteristics of HYNIC bioconjugates labeled using tricine as a coligand.

Using mass spectroscopic techniques, we have previously shown that when certain HYNIC–peptide conjugates are radiolabeled with ^{99m}Tc using tricine as a coligand, only 1 tricine molecule is involved in the complex, whereas typically 2 are observed (*5,9*). We speculated that this might be due to the coordination by neighboring amino acid side chains such as histidine or glutamic acid in the peptide sequence. We therefore investigated this phenomenon in a

series of model peptides and found that when histidine is located immediately adjacent to the HYNIC, the peptide showed markedly enhanced stability to cysteine challenge and bovine serum albumin (BSA) binding and contained only 1 tricine; peptides without histidine were less stable and contained 2 tricines (*10*).

We applied this finding to the design of peptides that could be used for imaging the clinically relevant cholecystokinin-2 (CCK-2) receptor to determine whether this assisted coordination resulted in improved performance and tumor targeting in vivo. We synthesized 3 peptide conjugates containing the –AYGWMDF-NH_2 C-terminal CCK-2 receptor–binding sequence, an N-terminal Lys(HYNIC) moiety, and an intervening sequence of potentially coordinating or noncoordinating amino acids. The peptides were radiolabeled with ^{99m}Tc/^{99}Tc using either tricine or EDDA as a coligand and analyzed by HPLC and liquid chromatography–mass spectrometric techniques. The stability in vitro was assessed by cysteine challenge and albumin binding, receptor binding and internalization by cell-binding studies, and in vivo targeting in AR42J-bearing mice by high-resolution SPECT/CT and biodistribution studies.

MATERIALS AND METHODS

Materials

The solvents used were of AnalaR (Merck) quality, and reagents were purchased from Aldrich-Sigma Chemical Co. unless stated otherwise and were used as received. $Na^{99m}TcO_4$ was obtained from a commercial ^{99}Mo/^{99m}Tc (Drygen; GE Healthcare) generator. ^{99m}Tc was obtained from Amersham International plc as solid ammonium pertechnetate; it was dissolved in water at a concentration of 2×10^{-4} M and passed through filter paper before being used.

Solid-Phase Peptide Synthesis (SPPS)

The 3 peptides studied (Fig. 1) were peptide 1: HYNIC (Lys)–Glu-Ala-Tyr-Gly-Trp-Met-Asp-Phe-amide; peptide 2: HYNIC (Lys)–Gly-His-Glu-Ala-Tyr-Gly-Trp-Met-Asp-Phe-amide; and peptide 3: HYNIC (Lys)–Gly-Ala-Tyr-Gly-Trp-Met-Asp-Phe-amide. All HYNIC–peptide conjugates were synthesized in the Biomolecular Analysis Laboratory, University of Kent, on a PSSM-8 Multiple Peptide Synthesizer (Shimadzu) using the conventional Fmoc strategy. Standard side-chain protecting groups were used (tyrosine: t-butyl; tryptophan: t-Boc; aspartate: *O*-t-butyl; and histidine: trityl), and the peptides were assembled on TGR amide resin (Novabiochem) using the *O*-(benzotriazol-1-yl)-*N,N,N′,N′*-tetramethyluronium hexafluorophosphate–mediated coupling approach. To incorporate the HYNIC group, at the appropriate juncture, Fmoc-(Boc-HYNIC)-lysine (*9,11*) was incorporated into the peptide as described above. The peptide was released from the resin, and side-chain Boc-deprotection was achieved by treatment with trifluoroacetic acid (TFA) containing 2.5% water and 2.5% triisopropylsilane. The peptide was isolated by precipitation in ice-cold diethyl ether and purified by HPLC. The product was dissolved in water and recovered by freeze-drying. Determination of peptide concentration was performed by ultraviolet (UV) spectroscopy at 280 nm using an extinction coefficient of 19,970 $mol^{-1} \cdot cm^{-1}$. Purity and identity were confirmed by HPLC and electrospray mass spectroscopy (ESMS).

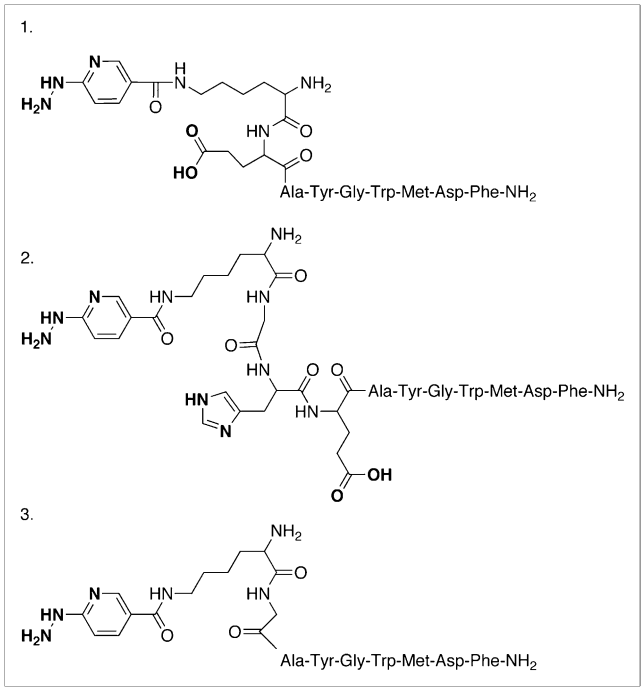

FIGURE 1. Structures of peptides used in this study. Peptide 1 is HYNIC (Lys)–Glu-Ala-Tyr-Gly-Trp-Met-Asp-Phe-amide; peptide 2 is HYNIC (Lys)–Gly-His-Glu-Ala-Tyr-Gly-Trp-Met-Asp-Phe-amide; and peptide 3 is HYNIC (Lys)–Gly-Ala-Tyr-Gly-Trp-Met-Asp-Phe-amide. Atoms shown in bold are potentially coordinating.

^{99m}Tc Labeling

Tricine. In a screw-top 2.5-mL polypropylene vial (Corning), 3 μg of HYNIC peptide in water were incubated with 0.5 mL of tricine solution (100 mg/mL in water), 0.5 mL of $^{99m}TcO_4^-$ solution (>200 MBq), and 10 μL of stannous chloride dihydrate solution (3 mg/mL in ethanol) for 30 min at 95°C.

EDDA. In a screw-top 2.5-mL polypropylene vial (Corning), 10 μg of HYNIC peptide in water were incubated with 0.25 mL of tricine solution (20 mg/mL in 0.4 M sodium dihydrogen phosphate), 0.25 mL of EDDA solution (10 mg/mL in 0.1 M sodium hydroxide [NaOH]; final pH 6.0), 0.5 mL of $^{99m}TcO_4^-$ solution (400–450 MBq), and 10 μL of stannous chloride dihydrate solution (3 mg/mL in ethanol) for 30 min at 80°C.

^{99}Tc Labeling

For liquid chromatography (LC)-ESMS and radioligand-binding analysis, the concentrations of reagents were increased.

Tricine. In a screw-top 2.5-mL polypropylene vial (Corning), 12.5 μg of HYNIC conjugate in water were incubated with 100 μL of tricine (100 mg/350 μL in water), 50 μL of $^{99}TcO_4^-$ solution (1×10^{-8} mol), 5 μL of $^{99m}TcO_4^-$ solution (3 MBq), and 5 μL of stannous chloride dihydrate solution (6 mg/mL in ethanol) for 30 min at 95°C.

EDDA. In a screw-top 2.5-mL polypropylene vial (Corning), 12.5 μg of HYNIC peptide in water were incubated with 50 μL of tricine solution (300 mg/mL in 0.35 M phosphate acid buffer, pH 4), 50 μL of EDDA solution (15 mg/mL in 0.1 M NaOH), 50 μL of $^{99}TcO_4^-$ solution (1×10^{-8} mol), 5 μL of $^{99m}TcO_4^-$ solution (3 MBq), and 5 μL of stannous chloride dihydrate solution (6 mg/mL

in ethanol) for 30 min at 80°C. Radio-HPLC and ESMS were performed to ensure that the increased concentrations of peptide and technetium did not significantly alter the identity of the labeled species formed (*5,9*).

Purification of Labeled Peptides

For purification of the radiolabeled peptide before stability and radioligand-binding studies, a solid-phase extraction method was used. A C18-Sep-Pak minicartridge (Waters) was first conditioned with 2 mL of methanol, washed with 5 mL of water, and dried with 5 cm^3 of air. The radiolabeling mixture was then passed through the cartridge and washed with 5 mL of water, and the radiolabeled peptide was eluted with 1 mL of 50% acetonitrile (ACN) and diluted for further study.

Radioanalytical Methods

Radiolabeled peptides were characterized by HPLC, instant thin-layer chromatography (ITLC), and LC-ESMS. A Beckman System Gold comprising a 168 diode-array UV detector (Beckman) and a radioactivity monitor (GABI; Raytest) and running 24-Karat proprietary software (Beckman) was used for reversed-phase-HPLC (RP-HPLC) analysis with a 30-nm column (250 × 4.60 mm, 5 μm) (Jupiter C18; Phenomenex). A flow rate of 1 mL/min and UV detection at 220–350 nm were used with the following gradient: ACN in 0.1% aqueous TFA: 0–5 min 0% ACN, 5–18 min 0%−25% ACN, 18–20 min 25% ACN, 20–25 min 25%−60% ACN, 25–30 min 60%−100% ACN, and 30–32 min 100%−0% ACN. ITLC was performed on silica gel (Gelman Sciences), with saline as an eluant for detection of ^{99m}Tc-pertechnetate and soluble nonpeptide-bound impurities (R_f = 1) and with 50% acetonitrile–water solution for determination of reduced hydrolyzed technetium (^{99m}Tc-colloid, R_f = 0).

LC-ESMS

ESMS was performed on 40–100 μL of the ^{99}Tc-carrier-added labeling mixture, prepared as described above, in both positive- and negative-ion mode using a Finnigan MAT LCQ ion-trap mass spectrometer coupled to a Hewlett-Packard 1100 HPLC system. HPLC parameters were as follows: Phenomenex Polymer PRP-1 column (150 × 2 mm, 5 μm); mobile phase: linear gradient of increasing ACN in 0.05% aqueous TFA: 0–5 min 5% ACN, 5–30 min 5%−90% ACN, 30–40 min 90%−100% ACN, and 40–45 min 100%−5% ACN; flow rate: 0.2 mL/min; and detection: UV absorbance at 214 and 254 nm. MS analysis of the HPLC eluate was performed using the following ESMS parameters: method A: peptide-analytic mode, negative-mode ionization with tube lens offset (skimmer), and capillary voltage set at −50 V and −16 V, respectively; method B: peptide-analytic mode, positive-mode ionization with tube lens offset (skimmer), and capillary voltage set at +30 V and +19 V, respectively; and method C: organic-analytic profile mode, positive-mode ionization with tube lens offset (skimmer), and capillary voltage set at 0 V and +15 V, respectively.

Cysteine Challenge

A total of 65 μL of purified ^{99m}Tc-labeled peptide and 70 μL of cysteine hydrochloride (50 mg in 100 μL of 0.1 M phosphate buffer) were mixed and incubated for 1 h at 37°C. The stability was assessed by RP-HPLC and ITLC as described above. The proportion of the total radioactivity associated with the HPLC peaks corresponding to the starting peptide complex was calculated.

BSA Challenge

A total of 10 μL of purified radioligand and 90 μL BSA (200 mg/mL in 0.1 M phosphate buffer) or 90 μL of 0.1 M phosphate buffer (control) were incubated for 3 h at 37°C. The percentage of radioligand bound to BSA was determined by centrifugation at 5,000 rpm for 1 min using size-exclusion columns (Microspin G-50; Sephadex). The retentate (nonbound) and eluate (protein-bound) were measured in a γ-counter (Compugamma 1282; LKB Wallac).

Radioligand-Binding Assay

AR42J cells were seeded at a density of 1×10^6 cells per well in 6-well plates (Nunclon) and grown for 24 h in 10% RPMI 1640 medium (Invitrogen) with 10% (v/v) fetal bovine serum medium. On the day of the experiment, cells were washed twice with ice-cold RPMI/1% (v/v) fetal bovine serum. The cells were supplied with fresh medium (1.2 mL) and incubated with approximately 200 fmol of the Sep-Pak–purified ^{99m}Tc-labeled peptide (150 μL in phosphate-buffered saline [PBS] corresponding to 1,000,000 counts per minute) and increasing concentrations (150 μL in PBS, 0.001–1,000 nM) of ^{99}Tc-labeled peptide in triplicate. The cells were incubated at room temperature for 2 h. Incubation was interrupted by the removal of the medium and rapid rinsing twice with ice-cold RMPI with 1% (v/v) fetal bovine serum medium. Thereafter, the cells were lysed by treatment in 1 mL of 1 M NaOH for 15 min. The supernatant was collected, and the wells were rinsed with 1 mL of PBS twice. The combined washings were measured in a γ-counter (Compugamma 1282; LKB Wallac).

Radioligand Internalization

AR42J cells were seeded in 10% RPMI/10% (v/v) fetal bovine serum medium at a density of 1×10^6 cells per well in 6-well plates (Nunclon) and grown for 24 h. On the day of the experiment, cells were washed twice with ice-cold RPMI/1% (v/v) fetal bovine serum. The cells were supplied with fresh medium (1.2 mL) and incubated with approximately 200 fmol of the ^{99m}Tc-labeled peptide (150 μL in PBS, corresponding to 1,000,000 counts per minute) and either 150 μL of PBS or 1 μM of unlabeled peptide (150 μL in PBS). The cells were incubated at 37°C in triplicate for 5, 15, 30, 60, and 120 min. Incubation was interrupted by the removal of the medium and rapid rinsing twice with ice-cold RPMI with 1% (v/v) fetal bovine serum medium. The cells were washed once with glycine buffer, pH 2.8 (50 mM glucose, 0.1 M sodium chloride), then twice with PBS to remove the surface receptor–bound fraction. Thereafter, the cells were lysed by treatment in 1 mL of 1 M NaOH for 15 min. The supernatant was collected, and the wells were rinsed 2 times with 1 mL of PBS. The collected fractions were counted in a γ-counter. The mean specifically internalized fractions were calculated in relation to the total activity added (percentage of total activity).

Radioligand Externalization

AR42J cells were treated as described for internalization experiments and incubated with the radioligand for 2 h. Incubation was interrupted by the removal of the medium and rapid rinsing twice with ice-cold RPMI/1% (v/v) fetal bovine serum, followed by an acid wash (with 50 mM glycine buffer, pH 2.8, 0.1 M sodium chloride) for 10 min to remove membrane-bound radioligand. The cells were supplied with fresh RPMI with 1% (v/v) fetal bovine serum alone or with 1 μM peptide 1 or peptide 2, at 37°C for 1 h of incubation. Incubation was interrupted by the removal and collection of the medium and rapid rinsing twice with ice-cold RPMI/1% (v/v) fetal bovine serum (externalized fraction). Finally, cells were lysed by treatment with 1N NaOH and collected (internalized

fraction). All fractions collected were counted in a γ-counter to determine the externalized and nonexternalized or retained fractions.

In Vivo Evaluation of Radioligands

All animal experiments were conducted in compliance with British Home Office regulations governing animal experimentation. Tumor xenografts were induced in female CD1 nude mice (Charles River) by subcutaneous injection of 10^7 AR42J cells, and the tumors were allowed to grow until they had reached a size greater than 0.7 mL (10–15 d). Biodistribution studies were performed as follows: ^{99m}Tc-labeled peptide (0.25 μg of peptide/10–12 MBq of ^{99m}Tc) was injected into the tail vein with or without the coinjection of 50 μg of the corresponding unlabeled HYNIC–peptide conjugate. Each mouse was measured in a suitable calibrated dose calibrator (CRC-15 Beta; Capintec) after injection. The mice were sacrificed in groups of 3 by cervical dislocation 1 h after injection. Tumors and other tissues (blood, stomach, spleen, liver, pancreas, kidneys, muscle, tail, and intestines) were removed and weighed. The tissues were counted in a γ-counter together with standards of known radioactivity, and the percentage injected dose per gram of tissue (%ID/g) was calculated by dividing the activity in the tissue samples (γ-counter) by the injected activity (dose calibrator). The unpaired *t* test (Excel; Microsoft) (significance level, 0.05) was used for statistical analysis. Imaging studies were performed using a NanoSPECT/CT small-animal scanner (Bioscan). ^{99m}Tc-labeled peptide (0.5 μg of peptide/20 MBq of ^{99m}Tc) was injected into the tail vein of AR42J-bearing CD1 mice. After 1 h, the mice were anesthetized with isoflurane (4% induction, 2% maintenance) and imaged using 36 × 1.4 mm pinholes acquiring 50,000–100,000 counts for each of the 16 projections. Radionuclide images were reconstructed using proprietary HiSPECT (Bioscan) iterative reconstruction and fused with CT images using proprietary InVivoScope (Bioscan) software.

RESULTS

The effects of the peptide sequence on the heterogeneity of the labeled species formed was explored using radio-HPLC (Fig. 2). When peptide 1 (lacking histidine) was labeled using tricine as a coligand, 2 main radiolabeled species were obtained (retention times, 20.05 and 20.6 min). An even greater level of heterogeneity was obtained using peptide 3. However, when peptide 2 (containing histidine) was labeled with tricine, a single major species (retention time, 21.5 min) was formed. When the peptides were labeled with EDDA as a coligand, a single major radiolabeled species was obtained in all 3 cases.

Mass spectroscopic analysis of the ^{99}Tc-labeled peptides was performed using LC-ESMS. Results are shown in Table 1. When labeled with tricine as a coligand, peptides 1 and 2 gave only peaks with masses that corresponded to 1 tricine molecule per technetium–peptide adduct. The masses observed were consistent with the addition of 1 technetium and 1 tricine molecule to the peptide, with the concomitant displacement of 5 protons. Peptide 3, on the other hand, gave peaks corresponding to both 1 and 2 tricine molecules binding to the technetium–peptide adduct, again with concomitant displacement of 5 protons. This pattern is consistent with that observed in our small-model complex studies (*10*).

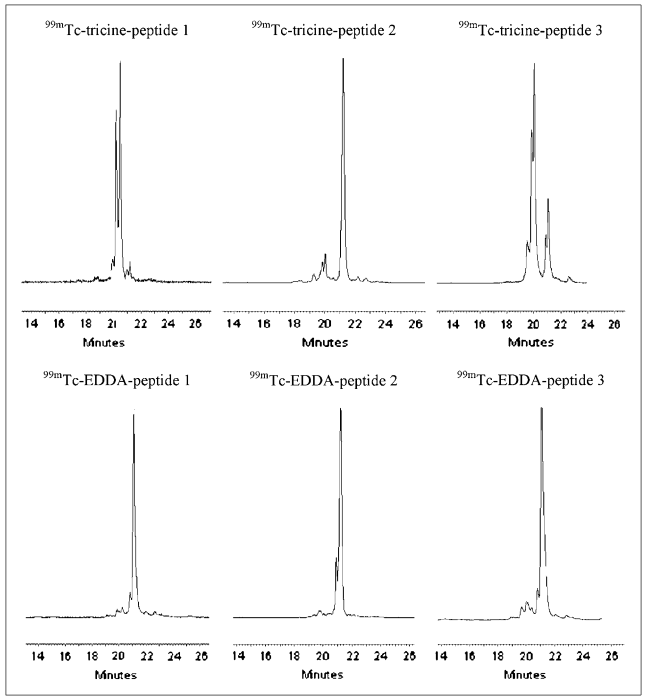

FIGURE 2. Radio-HPLC analysis of peptides 1–3 labeled using tricine and EDDA as coligands.

When labeled using EDDA as a coligand, both peptide 1 and peptide 2 gave adducts containing both 1 EDDA (minor species) molecule and 2 EDDA (major species) molecules.

The stability of the labeled peptides was studied in several ways: first, after a simple dilution in either PBS or human serum, and second, after challenge with either cysteine or albumin to measure the degree of transchelation to the cysteine or protein. The results of the dilution analysis are shown in Figure 3. When the peptides were labeled with tricine, the order of stability was peptide 2 > peptide 1 > peptide 3. When labeled with EDDA, all peptides showed enhanced stability, compared with their tricine counterparts, but peptide 3 still showed a lower stability than did peptides 1 and 2. The results of the cysteine challenge comparing the peptides labeled with tricine as a coligand are shown in Figure 4. There was no difference between peptides 1 and 2, but peptide 3 again showed a reduced stability. No difference was observed between the stability to cysteine challenge of the 3 peptides when labeled using EDDA as a coligand (data not shown). Also, no significant differences were identified in the trend of protein binding observed after challenge with albumin, whether the peptides were labeled with tricine or EDDA. All peptides showed protein binding in the range of 4%−9%.

The affinity of ^{99}Tc-labeled peptides 1 and 2 was tested using competition-binding assays on AR42J cells to determine their ability to compete with their corresponding ^{99m}Tc-labeled analogs (Table 2). All peptides exhibit an inhibitory concentration of 50% (IC_{50}) in the low nanomolar range, irrespective of whether they were labeled using tricine or EDDA as coligands. IC_{50} values in the same range were also

TABLE 1. Liquid Chromatography–Mass Spectrometric Analysis of ^{99}Tc-Labeled Peptides

Peptide	Molecular weight	Coligand	*m/z* [ES(+)]	No. of coligands/assignment	Retention time (min)
1	1,279.5	Tricine	1,553.3	[(1 + Tc + tricine – 5H)+H]$^{+}$	25.9; 26.0
			777.4	[(1 + Tc + tricine – 5H) + 2H]$^{2+}$	
		EDDA	1,548.2*	[(1 + Tc + EDDA – 5H) + H]$^{+}$	25.5 (minor)
			1,724.3*	[(1 + Tc + 2EDDA – 5H) + H]$^{+}$	27.0
2	1,473.5	Tricine	1,747.5	[(2 + Tc + tricine – 5H) + H]$^{+}$	26.2; 27.6
			874.5	[(2 + Tc + tricine – 5H) + 2H]$^{2+}$	
		EDDA	1,744.3	[(2 + Tc + EDDA – 5H) + H]$^{+}$	26.9
			873.4	[(2 + Tc + EDDA – 5H) + 2H]$^{2+}$	
			1,920.2	[(2 + Tc + 2EDDA – 5H) + H]$^{+}$	
			961.3	[(2 + Tc + 2EDDA – 5H) + 2H]$^{2+}$	
3	1,207.5	Tricine	1,481.3	[(3 + Tc + tricine – 5H) + H]$^{+}$	25.7–27.0
			741.5	[(3 + Tc + tricine – 5H) + 2H]$^{2+}$	
			1,660.5	[(3 + Tc + 2tricine – 5H) + H]$^{+}$	
			830.7	[(3 + Tc + 2tricine – 5H) + 2H]$^{2+}$	

All ES data are from positive-mode spectra, unless indicated with an asterisk.

obtained for the nonmetallated peptides. The rate of internalization of these ^{99m}Tc-labeled peptides in AR42J cells was also studied. When studied individually, all peptides showed a gradual increase in internalized activity over 2 h of incubation; however, a significant degree of interassay variability was seen as a result of changes in levels of expression of the CCK-2R in these cells. To overcome this source of variability, a direct comparison of each of the peptide–coligand combinations with an internal control (^{99m}Tc-EDDA–peptide 1) was performed. The results are shown in Figure 5. Despite a similar IC_{50} in the same cells, peptide 1 labeled with tricine showed a much lower degree of internalization than did the same peptide labeled using EDDA. With EDDA as a coligand, peptide 2 showed a greater degree of internalization than did peptide 1. Although peptide 2 showed a higher level of cell binding than did peptide 1, the proportion of externalized activity after 1 h for both ^{99m}Tc-EDDA–peptide 1 and ^{99m}Tc-EDDA–peptide 2 was similar (38% and 41%, respectively), values that are consistent with those observed for other ^{99m}Tc-labeled gastrin ligands (*12*).

The differences in rates of internalization were mirrored by significant differences in the biodistribution of the radiolabeled peptides in AR42J-bearing nude mice. The results are shown in Tables 3 and 4. The ^{99m}Tc-tricine–peptide 1 showed no significant receptor-mediated uptake, with high uptake by organs of excretion, in particular the kidneys and intestines. An in vivo study on ^{99m}Tc-tricine–peptide 3 was also performed, showing essentially identical biodistribution to peptide 1 (data not shown). When labeled with EDDA, peptide 1 showed a significant degree of receptor-mediated uptake in the tumor (half of which could be blocked by a coadministration of unlabeled peptide) and much lower accumulation in nontarget organs. Peptide 2 showed an improvement in tumor targeting over peptide 1. When labeled with tricine, the tumor uptake (one third of which could be blocked) was twice as high, and kidney and intestinal uptake were much reduced. When labeled with EDDA, the tumor uptake was enhanced and nontarget uptake reduced still further. These biodistribution results were reflected in the images obtained by NanoSPECT/CT (Supplemental Fig. 1; supplemental materials are available online only at http://jnm.snmjournals.org). A qualitative comparison of the images confirmed a hierarchical imaging performance of ^{99m}Tc-EDDA–peptide 2 > ^{99m}Tc-EDDA–peptide 1 > ^{99m}Tc-tricine–peptide 2 > ^{99m}Tc-tricine–peptide 1.

DISCUSSION

The aim of this study was to explore the influence of amino acid side chains on the coordination of ^{99m}Tc by HYNIC peptide. If the assisted coordination resulted in the formation of a more stable product, then that may result in improved receptor targeting and retention in vivo. On the other hand, if the assisted coordination resulted in a change in conformation of the peptide (which reduces its ability to bind to the receptor), then that would be likely to reduce the performance of the radiotracer in vivo. To explore this phenomenon, we designed and synthesized 3 peptides that contained a HYNIC moiety at the N terminus and the CCK-2R receptor–binding sequence at the C terminus, and we varied the amino acid sequence in between. Peptide 1 contained what is generally regarded as the minimum sequence required for high (low nanomolar) binding affinity to CCK-2R. This sequence (Glu-Ala-Tyr-Gly-Trp-Met-Asp-Phe-amide) also forms the basis of the peptide MG11, which has been widely studied (*13,14*). There is evidence from our previous studies that the glutamic acid side chain in this sequence is involved in the coordination of ^{99m}Tc (*5*). To release this glutamic acid from the coordination sphere, we synthesized peptide 2, which has an additional glycine–histidine spacer inserted between the CCK-2R binding motif and the HYNIC. Our previous studies indicate that the histidine would displace the glutamic acid from the coordination sphere and that the additional distance of the glutamic acid from the HYNIC

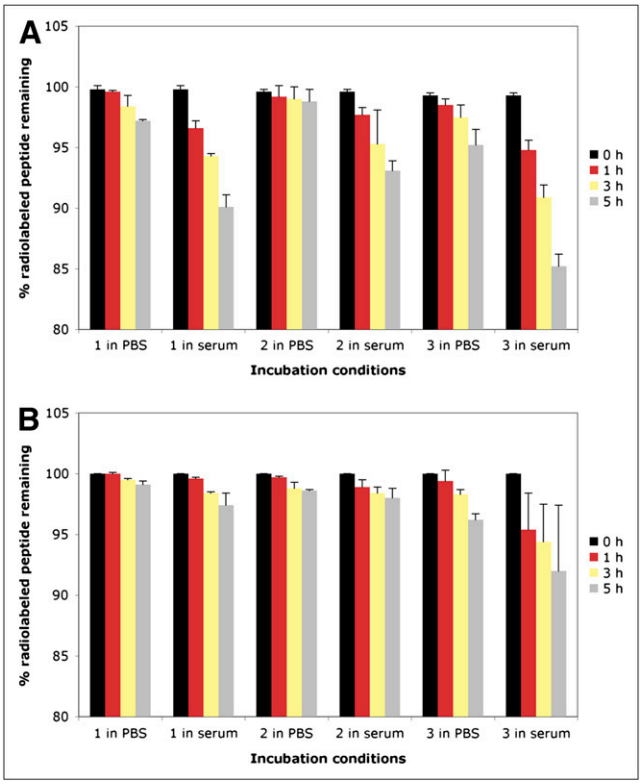

FIGURE 3. (A) Stability of ^{99m}Tc-peptides labeled using tricine as a coligand after dilution in PBS or human serum. (B) Stability of ^{99m}Tc-peptides labeled using EDDA as coligand after dilution in PBS or human serum.

would make it less likely to coordinate technetium. Both effects would make the glutamic acid more available for receptor binding but would also affect the requirement for coordination of the technetium by other coligands. Although our previous studies with short-model peptides suggested that the presence of either glutamic acid or histidine adjacent to the HYNIC results in a more stable complex, we wanted to confirm this finding with a clinically relevant peptide; we therefore synthesized peptide 3, in which the glutamic acid was replaced by a Gly that is not able to participate in the coordination of the radiometal.

The results obtained shed new light on the potential of ^{99m}Tc-HYNIC–peptide conjugates and the ability of sequence-specific amino acids to coordinate with the technetium atom. In general, the performance of peptides labeled using EDDA as a coligand is confirmed as superior to that of peptides labeled with tricine. EDDA forms more homogeneous preparations, with higher stability, ultimately resulting in improved tumor targeting in vivo. In addition, we showed that targeting performance can also be improved by incorporation of a histidine residue into the peptide sequence. This also results in a more homogeneous preparation with greater stability. However, this improvement in stability using histidine is observed only when combined with the relatively weak coligand tricine. With EDDA as a coligand, no improvement in homogeneity or stability in vitro was observed, and the number of coligand molecules incorporated into the complex remained unchanged. Nevertheless, peptide 2, compared with peptide 1, performed better in terms of cell internalization and in vivo tumor targeting, even when labeled with EDDA. This improvement is not due to any increase in receptor-binding affinity because this remains essentially unchanged. The presence of multiple histidine amino acids in a peptide has been shown to cause endosome disruption (*15,16*), which would perhaps result in enhanced egress from cells. However, we found no difference in the externalization of peptides 1 and 2, suggesting that the substitution of this single histidine residue does not have a similar effect. A further possible explanation is an improvement in stability in vivo that is not reflected in in vitro assays. The pKa of the cyclic amine in the histidine side chain is 6.0. Therefore, at the physiologic pH of 7.4, the majority of the residues will be uncharged and should not significantly affect the overall charge of the peptide in the blood. In an acidic environment, however, such as occurs within the lysosomal compartment, the net negative charge of the peptide will be reduced and this may affect intracellular metabolism. In a previous study, we found that the insertion of histidine can also enhance the performance of indium-

TABLE 2. Binding Affinity of $^{99m/99}$Tc-Labeled Peptides on AR42J Cells

Peptide–coligand combination	IC_{50} (nM)
$^{99m/99}$Tc-tricine–peptide 1	7.08 ± 0.83
$^{99m/99}$Tc-tricine–peptide 2	2.98 ± 0.37
$^{99m/99}$Tc-EDDA–peptide 1	7.48 ± 0.09
$^{99m/99}$Tc-EDDA–peptide 2	5.70 ± 0.30

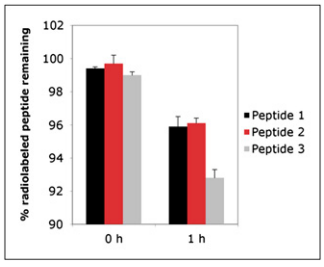

FIGURE 4. Stability of ^{99m}Tc-peptides labeled using tricine as coligand after challenge with cysteine.

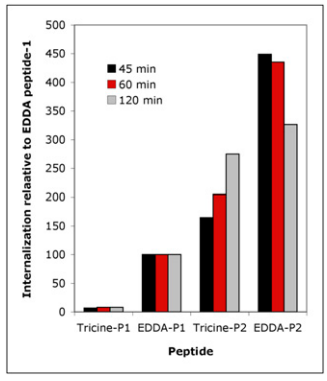

FIGURE 5. Internalization of ^{99m}Tc-labeled peptide 1 (P1) and peptide 2 (P2) labeled with tricine and EDDA as coligands. Internalization rates are expressed in relation to that seen with ^{99m}Tc-EDDA–peptide 1.

TABLE 3. Biodistribution of ^{99m}Tc-Peptides 1 and 2 Radiolabeled Using Tricine as Coligand in CD1 Nude Mice Bearing AR42J Tumor Xenografts at 1 Hour After Injection

	Peptide			
Organ	1	1 blocked	2	2 blocked
Liver	3.0 ± 0.7	7.6 ± 2.3	1.5 ± 1.3	2.2 ± 0.3
Kidneys	31.8 ± 5.1	35.9 ± 7.0	12.0 ± 1.6	19.1 ± 7.4
Tumor	0.8 ± 0.4	0.7 ± 0.20	1.7 ± 0.1*	0.6 ± 0.2
Blood	0.9 ± 0.2	1.4 ± 0.6	0.4 ± 0.1	0.6 ± 0.1
Stomach	0.5 ± 0.6	0.9 ± 0.8	1.1 ± 0.3	0.6 ± 0.1
Spleen	0.6 ± 0.1	1.5 ± 0.1	0.5 ± 0.4	0.6 ± 0.1
Intestine	5.9 ± 0.4	10.5 ± 2.2	1.0 ± 0.1	2.8 ± 0.5
Muscle	0.2 ± 0.1	0.4 ± 0.1	0.1 ± 0.0	0.1 ± 0.1
Pancreas	0.4 ± 0.1	0.4 ± 0.3	0.2 ± 0.0	0.2 ± 0.1

*Significant, $P = 0.05$.
Values are expressed as %ID/g (mean ± SD, $n = 3$).

1,4,7,10-tetraazacyclododecane-*N,N′,N″,N‴*-tetraacetic acid–labeled peptides (*17*), and this phenomenon is therefore worthy of further investigation.

Two other groups have explored the use of ^{99m}Tc-labeled minigastrin analogs in the nude mouse AR42J xenograft model. Von Guggenberg et al. have compared the biodistribution of peptides labeled using both the HYNIC and the tricarbonyl labeling systems (*18,19*), and Nock et al. have studied that of a tetraamine conjugate (*20*). However, most of these studies used peptides containing the gastrin pentaglutamate motif, which results in moderate increases in tumor uptake but high renal retention, compared with the truncated sequence studied herein (*17*). In our experience, caution should, in any case, be exercised in directly comparing results from different centers—even when apparently the same tumor cell line is used—because of differences in levels of receptor expression observed in different laboratories.

TABLE 4. Biodistribution of ^{99m}Tc-Peptides 1 and 2 Radiolabeled Using EDDA as Coligand in CD1 Nude Mice Bearing AR42J Tumor Xenografts at 1 Hour After Injection

	Peptide			
Organ	1	1 blocked	2	2 blocked
Liver	1.1 ± 0.3*	0.5 ± 0.2	0.4 ± 0.1	0.3 ± 0.0
Kidneys	10.1 ± 0.7	11.6 ± 1.7	10.3 ± 0.5	12.0 ± 2.4
Tumor	1.5 ± 0.6*	0.8 ± 0.1	2.6 ± 0.2*	0.8 ± 0.2
Blood	0.5 ± 0.1	0.5 ± 0.2	0.4 ± 0.0	0.3 ± 0.0
Stomach	1.9 ± 0.1*	0.4 ± 0.2	0.9 ± 0.5	0.4 ± 0.3
Spleen	0.5 ± 0.2*	0.2 ± 0.1	0.2 ± 0.0	0.1 ± 0.1
Intestine	1.1 ± 0.1	0.8 ± 0.3	0.6 ± 0.3	0.4 ± 0.3
Muscle	0.1 ± 0.0	0.2 ± 0.1	0.1 ± 0.0	0.1 ± 0.0
Pancreas	0.3 ± 0.0	0.2 ± 0.1	0.3 ± 0.0*	0.2 ± 0.0

*Significant, $P = 0.05$.
Values are expressed as %ID/g (mean ± SD, $n = 3$).

CONCLUSION

The insertion of potentially coordinating amino acids into the sequence of HYNIC–peptide conjugates for ^{99m}Tc labeling results in improved receptor-targeting performance. In the case of peptides labeled with tricine as a coligand, this increased performance is associated with improvements in the homogeneity and stability of the complexes formed. Enhancements in the performance of peptides labeled with stronger coligands such as EDDA may also be observed, even without an apparent improvement in stability.

ACKNOWLEDGMENTS

We thank Kevin Howland for assistance with the liquid chromatography–mass spectrometric analysis; Judith Hardy, of the University of Kent at Canterbury, and the peptide-synthesis unit of Cancer Research UK for the supply of the peptide conjugates; Julie Foster for her assistance with SPECT/CT image analysis; and all the members of the CRUK Nuclear Medicine Research laboratory for their support. This study was financially supported by EPSRC and Cancer Research UK.

REFERENCES

1. Decristoforo C, Mather SJ. Preparation, ^{99m}Tc-labeling, and in vitro characterization of HYNIC and N3S modified RC-160 and [Tyr3]octreotide. *Bioconjug Chem.* 1999;10:431–438.
2. Babich JW, Solomon H, Pike MC, et al. Tc-99m-labeled hydrazino-nicotinamide derivatized chemotactic peptide analogs for imaging focal sites of bacterial infection. *J Nucl Med.* 1993;34:1964–1974.
3. Liu S, Edwards DS, Looby RJ, et al. Labeling a hydrazino nicotinamide-modified cyclic IIb/IIIa receptor antagonist with Tc-99m using aminocarboxylates as coligands. *Bioconjug Chem.* 1996;7:63–71.
4. Abrams MJ, Juweid M, Tenkate CI, et al. Technetium-99m-human polyclonal IgG radiolabeled via the hydrazino nicotinamide derivative for imaging focal sites of infection in rats. *J Nucl Med.* 1990;31:2022–2028.
5. King RC, Surfraz MB, Biagini SCG, Blower PJ, Mather SJ. How do HYNIC-conjugated peptides bind technetium? Insights from LC-MS and stability studies. *Dalton Trans.* 2007;43:4998–5007.
6. Liu S, Hsieh WY, Kim YS, Mohammed SI. Effect of coligands on biodistribution characteristics of ternary ligand Tc-99m complexes of a HYNIC-conjugated cyclic RGDfK dimer. *Bioconjug Chem.* 2005;16:1580–1588.
7. Decristoforo C, Mather SJ. The influence of chelator on the pharmacokinetics of ^{99m}Tc-labelled peptides. *Q J Nucl Med.* 2002;46:195–205.
8. Babich JW, Coco WG, Barrow S, Fischman AJ, Femia FJ, Zubieta J. Tc-99m-labeled chemotactic peptides: influence of coligand on distribution of molecular species and infection imaging properties—synthesis and structural characterization of model complexes with the {Re(eta(2)-HNNC5H4N)(eta(1)-NNC5H4N)} core. *Inorg Chim Acta.* 2000;309:123–136.
9. Greenland WEP, Howland K, Hardy J, Fogelman I, Blower PJ. Solid-phase synthesis of peptide radiopharmaceuticals using Fmoc-N-epsilon-(Hynic-Boc)-lysine, a technetium-binding amino acid: application to Tc-99m-labeled salmon calcitonin. *J Med Chem.* 2003;46:1751–1757.
10. Surfraz MB, King RC, Mather SJ, Biagini SCG, Blower PJ. Technetium-binding in labelled HYNIC-peptide conjugates: role of coordinating amino acids [abstract]. *Eur J Nucl Med Mol Imaging.* 2007;34(suppl 2):S148.
11. Surfraz MB, King R, Mather SJ, Biagini SC, Blower PJ. Trifluoroacetyl-HYNIC peptides: synthesis and ^{99m}Tc radiolabeling. *J Med Chem.* 2007;50:1418–1422.
12. Behe M, Reubi J, Nock B, Mäcke H, Breeman W, Bernard H. Evaluation of a DOTA-minigastrin derivative for therapy and diagnosis for CCK-2 receptor positive tumours [abstract]. *Eur J Nucl Med Mol Imaging.* 2005;32(suppl):S78.
13. Trejtnar F, Laznicek M, Laznickova A, et al. Biodistribution and elimination characteristics of two ^{111}In-labeled CCK-2/gastrin receptor-specific peptides in rats. *Anticancer Res.* 2007;27:907–912.

14. Good S, Walter MA, Waser B, et al. Macrocyclic chelator-coupled gastrin-based radiopharmaceuticals for targeting of gastrin receptor-expressing tumours. *Eur J Nucl Med Mol Imaging.* 2008;35:1868–1877.
15. Kichler A, Mason A, Bechinger B. Cationic amphipathic histidine-rich peptides for gene delivery. *Biochim Biophys Acta.* 2006;1758:301–307.
16. Mason A, Leborgne C, Moulay G, et al. Optimising histidine rich peptides for efficient DNA delivery in the presence of serum. *J Control Release.* 2007;118:95–104.
17. Mather SJ, McKenzie AJ, Sosabowski JK, Morris TM, Ellison D, Watson SA. Selection of radiolabeled gastrin analogs for peptide receptor-targeted radionuclide therapy. *J Nucl Med.* 2007;48:615–622.
18. von Guggenberg E, Behe M, Behr TM, Saurer M, Seppi T, Decristoforo C. ^{99m}Tc-labeling and in vitro and in vivo evaluation of HYNIC- and (N_{α}-His)acetic acid-modified [D-Glu^1]-minigastrin. *Bioconjug Chem.* 2004;15:864–871.
19. von Guggenberg E, Dietrich H, Skvortsova I, Gabriel M, Virgolini IJ, Decristoforo C. ^{99m}Tc-labelled HYNIC-minigastrin with reduced kidney uptake for targeting of CCK-2 receptor-positive tumours. *Eur J Nucl Med Mol Imaging.* 2007;34:1209–1218.
20. Nock BA, Maina T, Behe M, et al. CCK-2/gastrin receptor-targeted tumor imaging with ^{99m}Tc-labeled minigastrin analogs. *J Nucl Med.* 2005;46:1727–1736.